14

Investigation of Road Surface Texture Wavelengths

Chengyi Huang and Shunqi Mei
Department of EME, Wuhan Textile University, Wuhan
P. R. China

1. Introduction

It is generally realized that pavement texture plays a vital role in the development of both pavement friction and tire wear. For the past several decades, pavement texture measurements and modeling analysis have attracted considerable interest of many researchers. Pavement profiles usually present many of the statistical properties of random signals, it is very difficult to distinguish the different surfaces through texture analyses. Based on ASTM E 867, pavement texture can be grouped into two classes micro- and macro-texture in terms of the deviations of pavement surface with characteristic dimensions of wavelength and amplitude. Pavement macrotexture has a substantial influence on the friction between tire and road surfaces, especially at high speeds and in wet pavement conditions. Kokkalis(1998) has shown a relationship between wet pavement accident rate and pavement macrotexture. As expected, the accident rate is reduced as macrotexture increases. Gunaratne et al. (1996) used an electro-mechanical profilometer to record the surface profiles made of asphalt and concrete. The data were later modeled using Auto Regressive (AR) models, where a Fast Fourior Transform (FFT) technique was used to graphically regenerate the pavement surface. Since the order of the models used in these studies was very low (AR(3)), they were able to only model macrotexture and could not capture the characteristics of microtexture. Fülöp et al. (2000) investigated the relationship between International Friction Index (IFI) and skid resistance and between IFI and surface macrotexture. It was found that the macrotexture relates to the hysteresis effects in the tire tread rubber and absorbs some of the kinetic energy of the vehicle. Hence, they concluded that macrotexture has a direct effect on skid resistance.

Today with the advance of measurement technology, by means of a sensor-measured texture meter, profile heights related to both microtexture and macrotexture can be obtained easily. Researchers have focused on the effect of microtexture on friction between the tire and the road surfaces. The investigations by Kokkalis (1998) classified the microtexture and macrotexture as the first and second order of pavement surface irregularities, respectively. Rohde (1976) demonstrated the importance of microtexture pattern as well as its amplitude on the load-carrying capability and the descent time of the tread element. Taneerananon and Yandell (1981) developed a model to simulate a rigid tread element sinking onto a cover of a road surface having microtexture and studied the effect of microtexture roughness on the braking force coefficient. They found that this effect becomes more important when the pavement surface is wet. Persson and Tosatti (2000) presented a comprehensive treatment of

the hysteric contribution to the friction for viscoelastic solids sliding on hard substrates with different types of (idealized) surface roughness. They discussed qualitatively how the resulting friction force depends on the nature of the surface roughness. It was found that, when rubber is slowly sliding on the surface, at velocity less than 1cm/s (as in the case to ABS-braking of automotive tires on dry and wet road surface), the rubber will deform and fill out the nanoscale cavities associated with the short-ranged surface roughness and this gives an additional contribution to the sliding friction.

With increase in number of vehicles and increase in speed limits and the subsequent traffic fatalities, tire-road friction estimation has become an important research issue with Department of Transportation (DOT). In particular, researchers have paid more attention to the investigation of elevation road surface texture as a function of Average Daily Traffic (ADT). In the first part of this article, to further understand the features of polishing process on pavement surfaces, experimental texture measurements and Data Dependent Systems (DDS) approach were utilized to model and analyze the elevation profiles collected from polished and unpolished aggregate surfaces of Aggregate Wear Index (AWI) wear track. A key problem in texture measurement was how to determine sampling step sizes so as to reveal the properties of tire polishing process. Three step sizes were adopted to measure the aggregate surfaces. The DDS approach was then used to model and analyze those elevation profiles collected from polished and unpolished AWI wear track surface. It was found that the DDS approach was able to capture both the characteristics of the evolved macrotexture and microtexture and the polishing effect on the aggregate surfaces is found to reduce the microtexture roughness significantly. The second part in this article is to exhibit a texture analysis from several bituminous pavement surfaces obtained from Michigan, USA. Since traffic abrades the pavement surface, exposing aggregates and makes aggregates worn and polished, the polishing properties of coarse aggregates play a significant role in determining skid resistance. Therefore, 1 micron step size scan was used to collect the elevation profile from exposed aggregates and 45 micron step size scan was arranged to collect data from texture surface on each core surface, respectively. DDS approach was utilized to model and analyze the data for both 1 micron and 45 micron step size scans. The characteristics of both microtexture and macrotexture were derived by applying different criteria to DDS modeling analysis and they were correlated to the British Pendulum Tester numbers (BPNs) Laboratory Friction Tester values (LBF) and obtained on the same core. A good correlation was found from some mixed type of pavements.

2. Surface texture measurements

In order to simplify the analyses of road surfaces, aggregate surface textures on AWI wear track were investigated first. Figure 1 shows several polished aggregate on a portion of the AWI wear track obtained from Michigan Department of Transportation (MDOT). Since 1971, MDOT has been using a laboratory wear track to quantify the tendency of individual coarse aggregate sources to polish under the action of traffic (Dewey, et. al., 2001). The wear track consists of a pair of diametrically opposite wheels each attached to a common center pivot point. An electric motor is used to apply a driving force to the wheels through the center pivot point. The aggregate test specimens used on the wear track are trapezoidal in shape. Uniformly graded aggregates are placed in a layer directly against the mold and then covered by portland cement mortar. When 16 of the test specimens are placed end to end, they form a circular path about 2.13 meter in diameter. The surface of the wear track is consisted of limestone aggregate (from Port Inland, MI) of around 10mm size.

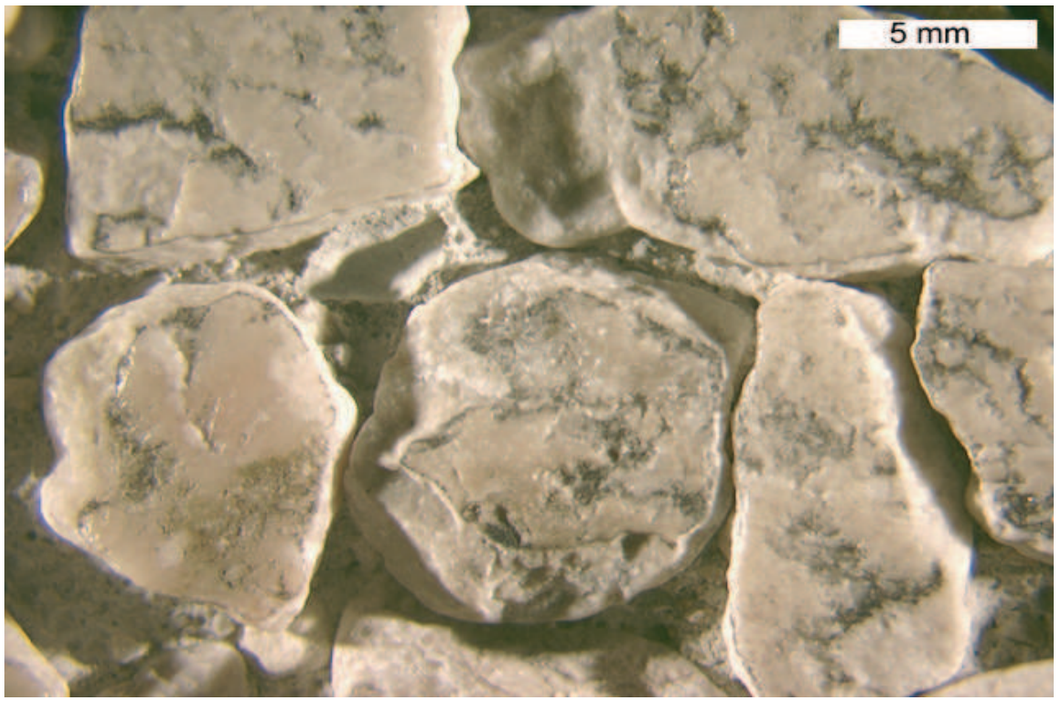

Fig. 1. Polished AWI wear track surface

The purpose of this section is to characterize the macrotexture and the microtexture present on both the polished (smooth) and the rough (unpolished or original) AWI aggregate surface. A laser profilometer was used to collect the elevation profiles on the surfaces. The profilometer can scan a 50.8×50.8 mm square area on any given sample surface. However, due to the restriction on the number of data points that can be effectively used in the subsequent DDS analysis, a maximum of 1024 points were collected for each scan length. Therefore, higher resolution scans were used for short scan lengths and vice versa. For example, if one micron step size is adopted to scan a surface, then the maximum scan length allowed is around one millimeter, in which the scan included 1024 data points.

Since the optimum step size for a given pavement is not known a priori, a number of step sizes (from 1 micron in Do, et. al.,(2000) to 20 millimeters in Perera, et. al., (1999)) have been chosen to measure road surface irregularities. Most of the texture measurements were characterized by Mean Texture Depth (MTD) (Gunaratne, et. al., (1996)) or Root Mean Square (RMS) of texture profile (Fülöp, et. al., 2000). Those measurement analyses seemed to have a good relationship with other road surface friction tests. In this paper, three step sizes, 1micron, 30micron and 45micron, were chosen to scan both the smooth and rough aggregate surfaces spanning 1mm, 7mm and 45mm, respectively. Typically, the 1μm and 30μm scans were limited to one aggregate surface and hence can provide the microtexture present on the individual aggregate, whereas the 45μm scans sampled several aggregates and the spaces in between, and therefore, were able to capture the features of both macrotextural and microtextural features of the wear surface. In addition, the 30micron scans can also provide a criterion for distinguishing between polished and unpolished aggregate surfaces for large scan step size. A total 10 scans were collected for each step size, 5 from polished surfaces and 5 from unpolished surfaces. Each scan data was imported into a DDS program so that parameters of the model such as frequency, wavelength, damping ratio and variance

contribution could be determined. Comparisons of the model parameters from the polished and unpolished scans can reveal the differences between them.

3. Data Dependent System (DDS) methodology

DDS approach is commonly used for time series analysis of sequentially sampled data. The methodology provides an effective approach to model such series in a statistically optimal manner. The elevation profile collected by the laser profilometer is essentially a uniformly sampled time series or space series data. The DDS modeling of the texture of the aggregate surface is aimed at a complete frequency or wavelength decomposition of the surface.
The DDS approach for modeling the elevation profiles utilizes the Autoregressive Moving Average model, represented as ARMA(2n,2n-1) (Pandit and Wu, 1983) and is given by

$$X_t = \varphi_1 X_{t-1} + \varphi_2 X_{t-2} + \cdots + \varphi_{2n} X_{t-2n} + a_t - \theta_1 a_{t-1} - \theta_2 a_{t-2} - \cdots - \theta_{2n-1} a_{t-2n+1} \quad (1)$$

where the variable X_t denotes the "state" of a system at time t, i.e., the profile height in this analysis. The adequacy of the model implies that a single state X_t completely characterizes the behavior of the system by expressing the dependence of the present state, i.e., the current profile height X_t on past states X_{t-1}, X_{t-2}, …, X_{t-2n}. The remainder a_t's are independent or uncorrelated random variables with zero mean and are often called as white noise. The order n of the model is increased until an adequate model is found, which will be explained later. In Eq. (1), the φ_i's are autoregressive parameters.
If the ARMA(2n, 2n-1) model is adequate, the roots λ_i (i=1, 2, 3,…, 2n) can be found from the characteristic equation

$$\lambda^{2n} - \varphi_1 \lambda^{2n-1} - \varphi_2 \lambda^{2n-2} - \cdots - \varphi_{2n} = 0 \quad (2)$$

where a real root provides a decaying exponential dynamic mode and a complex conjugate pair of roots provide a decaying (damped or undamped) sinusoidal mode with certain decay rate and frequency or wavelength. Using the backshift operator $BX_t = X_{t-1}$,

$$X_t = \frac{1 - \theta_1 B - \theta_2 B^2 - \cdots - \theta_{2n-1} B^{2n-1}}{(1-\lambda_1 B)(1-\lambda_2 B)\cdots(1-\lambda_{i-1}B)(1-\lambda_i B)(1-\lambda_{i+1}B)\cdots(1-\lambda_{2n}B)} a_t = \sum_{j=0}^{\infty} G_j a_{t-j} \quad (3)$$

where

$$G_j = g_1 \lambda_1^j + g_2 \lambda_2^j + \cdots g_{2n} \lambda_{2n}^j \quad (4)$$

is called as Green's function and the coefficients corresponding to the root λ_i are given by

$$g_i = \frac{\lambda_i^{2n-1} - \theta_1 \lambda_i^{2n-2} - \cdots - \theta_{2n-1}}{(\lambda_i - \lambda_1)(\lambda_i - \lambda_2)\cdots(\lambda_i - \lambda_{i-1})(\lambda_i - \lambda_{i+1})\cdots(\lambda_i - \lambda_{2n})} \qquad i = 1,2,3,\cdots 2n \quad (5)$$

The g_i terms simply scale the magnitude of the response from the ith mode and can also introduce a phase shift when that mode is sinusoidal . To better clarify the role of complex conjugate pairs of roots, each λ_i, λ_i^* and associated g_i, g_i^* can be expressed in the form of

$$g_i \lambda_i^j + g_i^* \lambda_i^{j*} = 2|g_i||\lambda_i|^j \cos(\omega_i j + \beta_i) \quad (6)$$

where the damped frequency ω_i and phase shift β_i come from the root λ_i and the corresponding scaling factor g_i respectively (Pandit and Wu, 2001). The damped frequency can further be expressed in terms of the damping ratio ζ and natural frequency ω_n as

$$\omega_i = \omega_n \sqrt{1-\zeta^2} = \cos^{-1} \frac{\mathrm{Re}(\lambda_i)}{|\lambda_i|} \tag{7}$$

where the damped angular frequency ω_i and the natural frequency ω_n are expressed as angle per sampling interval, and can be converted into cycles per second (Hz) by dividing 2π or can be converted into wavelength by using the constant speed of the profilometer. For a real root, the break or pseudo-frequency defined by the half power point in the spectral domaine.

Once the model has been fitted to the corresponding elevation profile data, the variance can be written in terms of the roots as

$$\gamma_0 = Variance(X_t) = E(X_t^2) = d_1 + d_2 + \cdots + d_{2n} \tag{8}$$

where

$$d_i = \sigma_a^2 \sum_{j=1}^{2n} \frac{g_i g_j}{1-\lambda_i \lambda_j}, \qquad i = 1,\ 2, \cdots,\ 2n \tag{9}$$

Thus, the power of a particular root, that is its contribution to the variance $\gamma_{0,}$ is represented by the corresponding d_i.

The choice ARMA(2n,2n-1) sequence is mainly based on the configuration of the characteristic roots λ_i. Since the autoregressive parameters φ_i's are always real, the complex roots can occur only in conjugate pairs. For example, for an ARMA(2,1) model, we have

$$(1-\varphi_1 B - \varphi_2 B^2) = (1-\lambda_1 B)(1-\lambda_2 B)$$

$$\lambda_{1,}\ \lambda_2 = \frac{\varphi_1}{2} \pm \frac{\sqrt{\varphi_1^2 + 4\varphi_2}}{2}$$

and

$$\kappa_1 = \lambda_1 + \lambda_2, \qquad \varphi_2 = -\lambda_1 \lambda_2 \tag{10}$$

If $\varphi_1^2 + 4\varphi_2 < 0$, then the roots λ_1 and λ_2 must be a complex conjugate pair. Therefore, if we increase the order by one, allowing odd autoregressive orders, one of the roots will be forced to be real. Another reason is that increasing the autoregressive order in steps of two is more economical than in step of one. One fits only half the number of models compared to the increase by step of one.

Using the above formulation, the experimentally obtained elevation profiles for each scan were modeled. The critical issue in modeling is to identify the correct model order $2n$, that completely captures the trends (or correlations) in the experimental data. To achieve this, the model order is continuously increased until the adequate order of the model is determined based on three criteria (Pandit and Wu, 2001): (1) Verify the independence of the residuals (the a_t's) of the fitted model by using the autocorrelations of the residuals, i.e., the chosen model is deemed to completely charaterize the data if the unified correlations (sample correlation divided by its standard deviation) are less than two which correspond to 95% probability in a normal distribution; (2) Once the data have been characterized

completely, the residual sum of squares (RSS) is made as low as possible by introducing an F-test parameter that relates the RSS from the current model order 2*n* to the previous model order (2*n*-1) in the computer program. The F-test parameter value is smaller value than the one from an F-table corresponds to a statistically insignificant reduction in RSS; (3) The adequate model should capture an obviously known physical frequency, such as the one corresponding to the size of aggregate on the surface.

4. Analysis of polished and unpolished aggregate surface profiles

4.1 One micron step size scan

Figures 2a and 2b present two typical elevation profiles collected at 1micron step size from polished and unpolished surfaces of AWI wear track, respectively. Clearly, the vertical scale in these two plots indicates that the magnitudes of the elevations are significantly different in both the data, and hence the variance (averaged square deviation from the mean) is essentially higher for the unpolished surface compared to that on the polished surface. The unpolished scan also appears to have a more complicated profile than the polished scan. This is an important physical characteristic that will be utilized in interpreting the model order in the following DDS analyses.

The data for each scan from the polished and unpolished surfaces was modeled by the DDS program. The starting model for every scan was ARMA(2,1) and the model order was increased in steps of 2, until the adequate model that satisfies the three criteria mentioned above was found. Table 1 and Table 2 present the modeling results for the two scans in Figures 2a and 2b respectively, with adequate models ARMA(12,11) (for 01a polished profile) and ARMA(22,21) (for 011 unpolished profile), respectively. Note that since unpolished scan is generally more complicated than polished one, the adequate model for unpolished scan usually has a higher order compared to that of the polished surface. In these tables, the frequency refers to number of cycles per millimeter. The wavelength is the inverse of this spatial frequency. The damping ratio indicates how well a given wavelength component of the profile repeats at that frequency in the scan. For example, a damping ratio of zero indicates a perfect sinusoidal wave extending for infinite time or length. The maximum damping ratio tending to unity implies that the wavelength component does not repeat at all. In Figure 2a, there exits a dominant peak that shows up at half shape of a wave crest at the end. Generally, the dominant peak has the largest height and the largest wavelength compared to other wave crests or wave troughs, may not repeat in the same elevation profile and will show up as a real root with very large wavelength in DDS analysis. The DDS analysis can capture these features effectively. For 1mm scan, this dominant peak also provides a way to distinguish the difference between polished and unpolished surfaces in the DDS analysis. These dominant peaks are indicated by bold in the Tables. In Table 1, the dominant wavelength is 0.433839mm and the corresponding variance contribution is 2.01E-4 mm^2, which is less than the dominant contribution of 1.42E-3 mm^2 from the unpolished scan in Table 2. All other wavelengths given in these tables are significantly smaller with low variance contribution and typically have much smaller damping ratio indicating that these wavelengths repeat over a long period time. Thus, the 1mm scans capture the microntextural features effectively.

Table 3 presents the modeling results from 10 scans. It is clear that both the variances and the dominant variance contributions for unpolished surfaces are consistently larger compared to those of the polished surfaces. Comparison of the dominant wavelengths

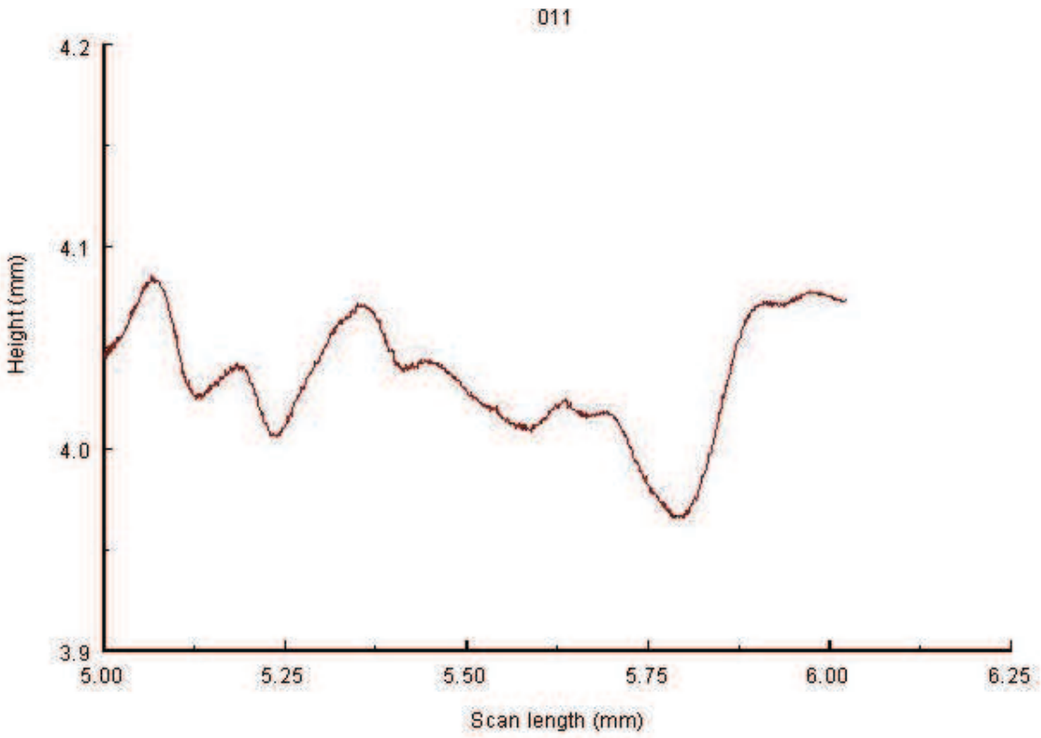

Fig. 2a. 1 micron scan from polished aggregate surface

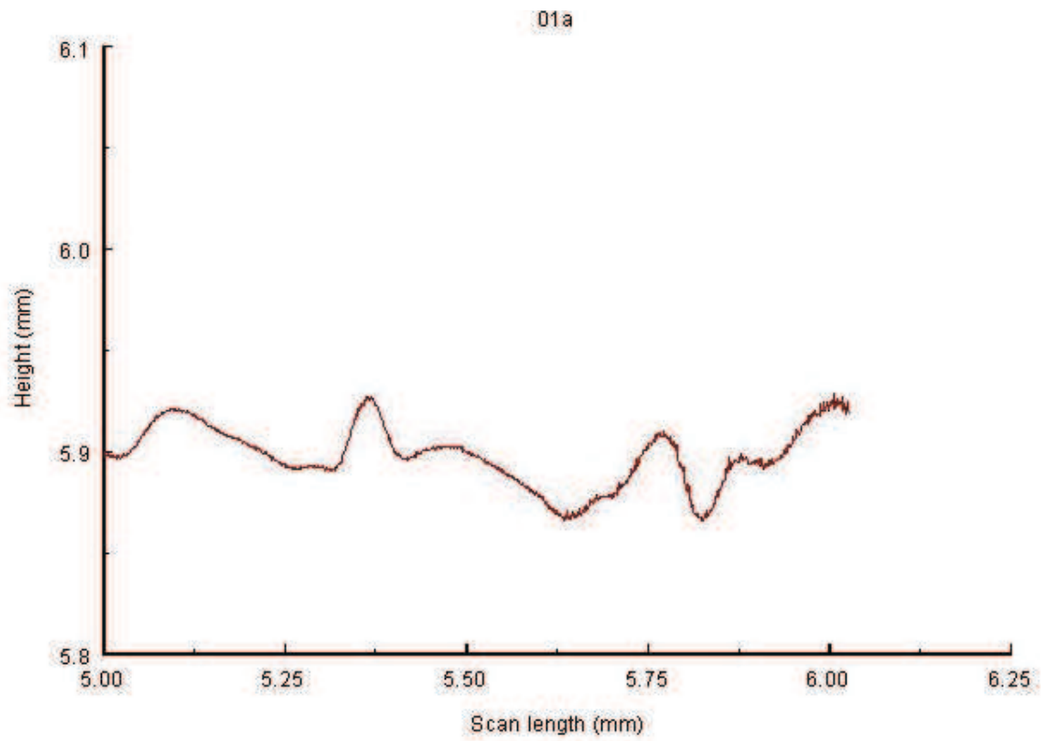

Fig. 2b. 1 micron scan from unpolished aggregate surface

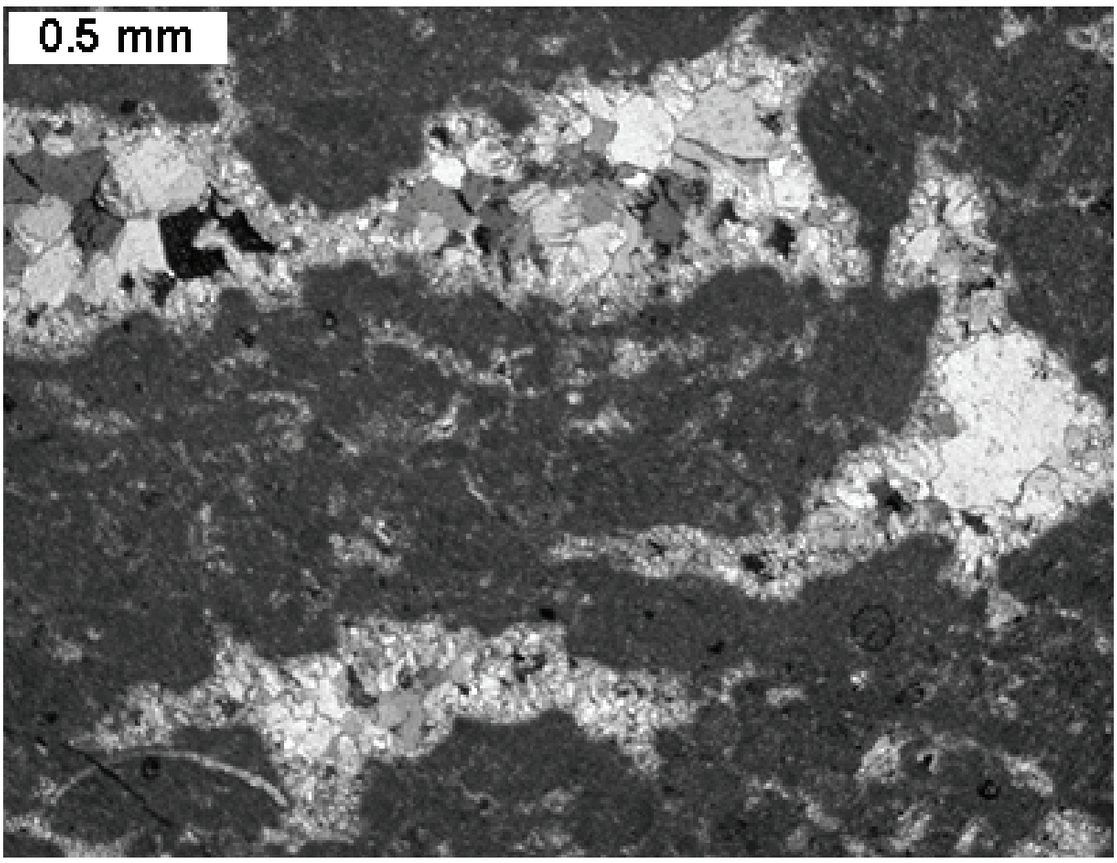

Fig. 3. Microstructure of Port Inland aggregate

obtained from the polished and unpolished surfaces reveals that these wavelengths do not present any trend implying that the tire polishing did not change the dominant wavelengths but only the overall variance contribution. Further analysis of Port Inland aggregate reveals that the dominant wavelengths have a strong relationship with the grain size of the aggregate. The grain size of the Port Inland aggregate used in this AWI wear track is usually in the range of 100micron to 500micron and this range seems to agree well with the dominant wavelengths in Table 3. Figure 3 presents the microstructure of Port Inland aggregate (The dark area is composed of algae lumps and they have a very fine grain size around of 2-10 micron, the white area is composed of calcite crystals with grain size around 20-500 micron). It is worth mentioning that for other shorter wavelengths, no trend can be found from the corresponding contributions when comparing between polished and unpolished aggregate surfaces is made. Therefore, the dominant wavelengths are the minimum wavelengths that can provide a trend between the polished and the unpolished aggregate surfaces in 1mm scans.

4.2 Thirty micron step size scan

In order to explore the effect of other larger wavelengths on the roughness of aggregate surfaces, 30 micron step size scans were collected from smooth and rough aggregate surfaces (5 scans from polished, 5 scans from unpolished). Because of the limited size of each aggregate, the 30 micron step size scans were composed of only 234 sampling points

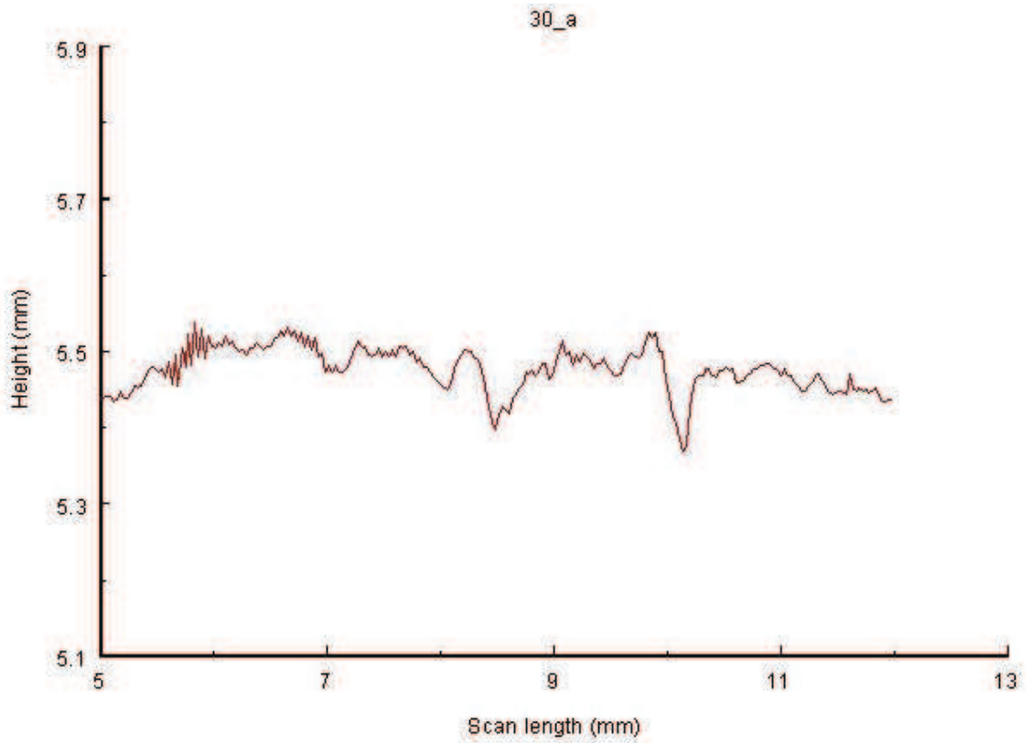

Fig. 4a. 30 micron scan from polished aggregate surface

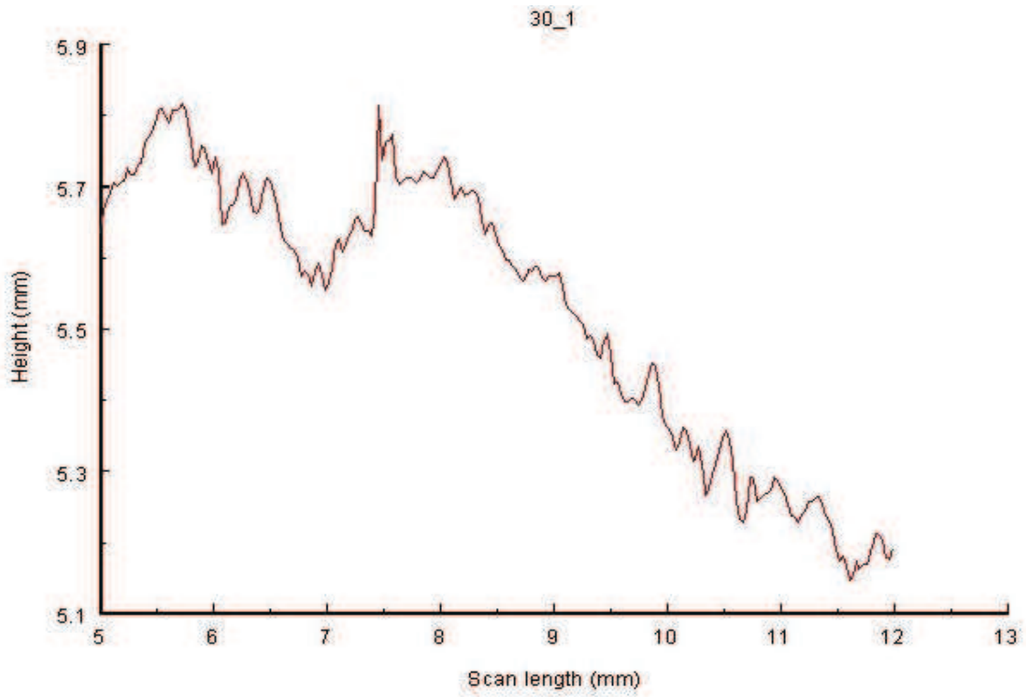

Fig. 4b. 30 micron scan from unpolished aggregate surface

extending over 7.02mm in length and were limited to one aggregate surface. Figures 4a and 4b present two typical elevation profiles collected from polished and unpolished surfaces. Similar to the 1micron step size scans, the vertical scale in these two plots indicates that the magnitudes of the elevations are significantly different and hence the variance of unpolished scan is essentially higher than that of the typical polished scan. However, since aggregate surface is not a flat plane naturally, even on the fully polished surface there still exist some significant irregularities where the tire rubber neither could contact aggregate surface entirely nor polish to reduce the height of irregularities. Figure 4a presents the situation where there are two large wave troughs that are hardly affected by the tire polishing action. These kinds of troughs may become the dominant wavelengths and affect the variance of elevation profiles significantly.

Another feature that affects the value of variance contributions may come from a slope in an elevation profile. In Table 4 and 5, the values of variance seem to present a trend between polished and unpolished surfaces. However, in Table 5, there are two real roots, one at 1.293mm and the others at 82.44mm wavelength. The dominant wavelength of 82.44mm is 11.7 times the scan length. This indicates that there is a slope in the overall elevation profile (Figure 4b) which has been effectively captured by the DDS program. Even in a 1mm scan, if a slope exits for the overall scan, a dominant root will reflect that feature. However, by carefully selecting a small flat region, likelihood of such a slope in a 1mm scan can be minimized. This can not be done in a 30mm scan, therefore, the value of variance does not present a criterion to distinguish the polished and unpolished surfaces. This can also be confirmed by the variance values in Table 6, where the variances are of comparable order between polished and unpolished aggregate surfaces. Therefore, the criterion used in 1micron step size scans to distinguish the difference between rough and smooth scans is not applicable to 30micron step size scans.

Usually, if the damping ratio is less than 10%, Eq. (7) shows that the frequency is nearly undamped and the component repeats regularly. Its contribution to the variance is given by Eq.(8) as d_i for a real root λ_i and $d_i + d_{i+1}$ for a complex conjugate pair λ_i, λ_{i+1}. Since a 30micron step size scan is 7 times the scan length of 1micron step size, it is possible that the dominant wavelength in 1micron step size scan may also appear several times in 30micron step size scans. Therefore, a new criterion based on damping ratio is introduced in 30micron step size scan analyses, i. e., contributions from all the wavelengths that have a damping ratio less than 10%, (see the column "criterion" in Table 4 and 5) are summed up to obtain a partial contribution (see the column "partial" in Table 4 and 5). Table 6 presents those partial contributions obtained from 10 such scans as well as the variation ranges of corresponding wavelengths. Since most of the wavelengths are less than 0.5mm, the texture can be depicted as 'microtexture' and the associated partial contributions physically describe the averaged squared microtexture roughness. In Table 6, there are two 'negative' partial contributions; the negative signs imply that these contributions have phase opposite to those with positive contribution. Comparison of the partial contributions between the polished and unpolished surfaces clearly indicates that polished aggregate line scans have significantly lower 'partial contributions' than those on the unpolished scans. This means that polishing wears away the micro-roughness present on the original aggregate surfaces. It is also interesting to note that the microtexture wavelengths satisfying the damping ratio criterion in 30micron step size are close to the dominant wavelengths in 1micron step size. Thus, both 1micron and 30micron step size scans capture the microtextural features effectively. Another interesting

feature is that the microtexture wavelengths in the polished scan have a much smaller range and smaller wavelengths than in the unpolished scans. This means that the polishing effect is to either chip away or break the larger grains from the original surface due to the traffic.

4.3 Forty-five micron step size scan

In the above 1micron and 30micron step size analyses, the characteristics related to macrotexture have not been found. The reason is that 1micron or 30micron scan lengths are too short and span only one aggregate. Therefore, 45micron step size scan was adopted which spans over 45mm length encompassing several aggregates. Figure 5a and 5b present two typical elevation profiles collected at 45micron step size from polished and unpolished surfaces, respectively. It is clear that there are several profiles of aggregate in the two plots and they all have an average size of around 10 millimeters. Comparison of two elevation profiles reveals that the scans obtained from unpolished aggregate surfaces appear to be rougher than those from the polished surfaces. Also, due to the inherent irregularities present on any aggregate surface, they do not get polished uniformly. Hence every scan includes some portion of unpolished surface. This will increase the complexity of DDS model analysis.

It is required to choose every scan line carefully so as to reduce the rough portions included in any given scan on a polished surface.

Table 7 and Table 8 present the modeling results corresponding to Figure 5a and 5b, respectively. Note that the model order is significantly smaller for polished scans compared to that of unpolished scans. The dominant contributions correspond to the largest wavelengths in these tables are 10.4 mm and 6.64 mm, respectively resulting from real roots.

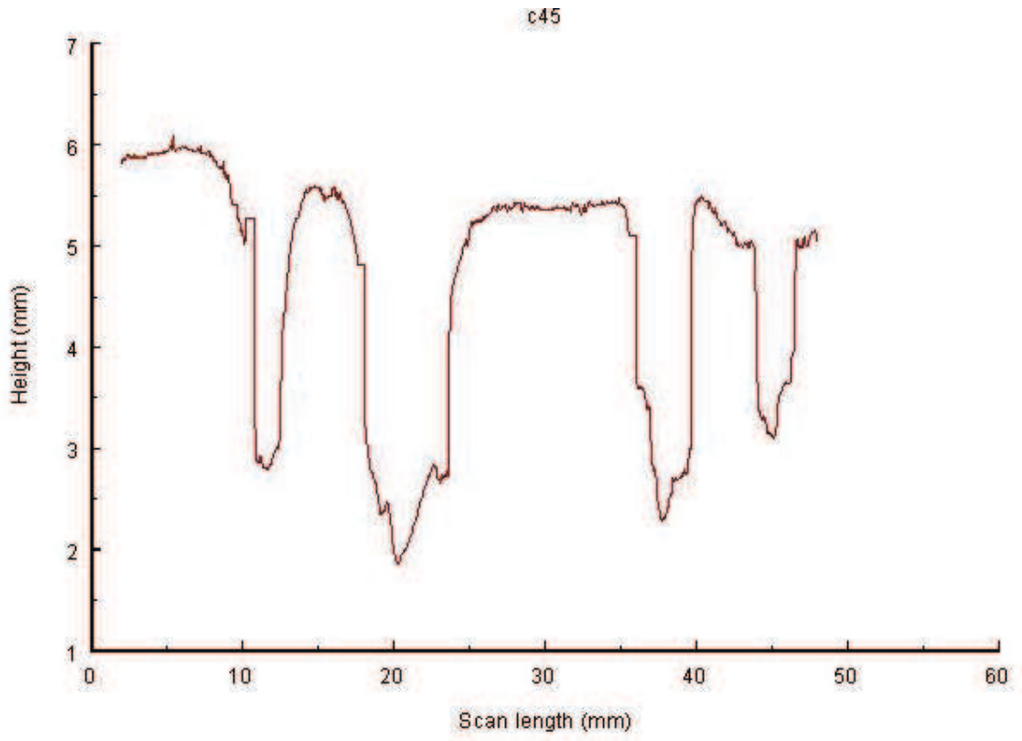

Fig. 5a. 45 micron scan from polished aggregate surface

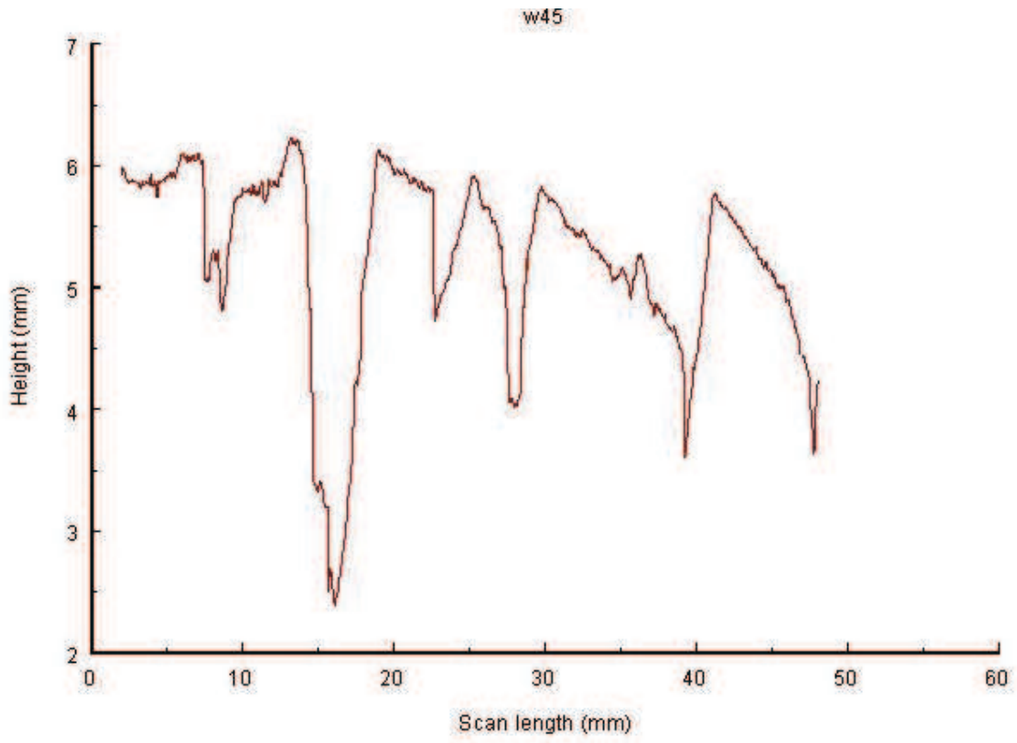

Fig. 5b. 45 micron scan from unpolished aggregate surface

These two wavelengths indicate physically the average size of the aggregates appearing in Figure 5. Considering the two tables, except for the largest wavelengths, the other wavelengths appear to be in the range of microtexture varying from 0.1mm to 0.5mm. It is once again verified that polishing the aggregate surface dose not change the wavelengths in the microtexture. To determinate contributions, the same criterion based on damping ratio as depicted in 30micron step size scans was used to distinguish the contributions between smooth and rough aggregate surfaces. It can be found from the tables that, when the value of 'damping ratio' is less than 0.1, the corresponding wavelengths are always less than 0.5mm, and these wavelengths agree well with the dominant wavelengths in 1micron step size scans or the grain size on aggregate surfaces. Therefore the characteristics of the microtexture can be captured by prescribing the small damping ratio criterion and the corresponding contribution describes the microtexture roughness. Comparing the two tables, it is clear that the polished surface has a smaller partial contribution (of the order of around 10^{-7}) and the unpolished one has a higher partial contribution (of the order of around 10^{-4}). Therefore, it appears that polishing reduces the microtexture roughness, but does not change the microtexture wavelengths significantly.

Table 9 summarizes the modeling results from 10 scans. It is clear that the variance does not show any trend between polished and unpolished surfaces. This is expected because of the large contributions that arise from the aggregate surfaces and spaces (troughs) in between the aggregates in addition to any contribution that may arise from any slope of the overall surface. These features completely mask the minor contributions arising from the polished regions. However, the partial contributions that are based on 10% damping ratio criterion reveal a clear trend between polished and unpolished surfaces, where the unpolished surface scans have contributions of the order 10^{-3} to 10^{-4} and the polished surface scans have

contributions of order 10^{-4} to 10^{-7}. However, the range of microtexture wavelengths as well as their overall values is significantly smaller on the polished surfaces indicating that the polishing effect due to traffic is to either chip away the large particles (or grains) or break them into smaller fragments.

As mentioned in the introduction, most of the previous publications in the literatures have focused on obtaining a single number either in terms of MTD or RMS to distinguish between polished and unpolished surfaces. Although, such a size single number is desirable for simplicity, it can not provide a more in-depth description of the micro- as well as macro-textural features that are characteristics of any polishing process. Moreover, comprehensive descriptions of the evolving wavelengths are desirable for more precise correlations with any other laboratory of field measurements such as British Pendulum Number (BPN) or field friction number (FFN) on pavements. Characterization of the evolving micro-texture is also essential for identification of the wear mechanisms on a given aggregate surface due to the type or the level traffic, type of mix-designs and age of pavement, the weather conditions over a period of time or a combination of the above.

However, the aim of the current paper is to introduce a methodology that can be effectively used on aggregate surfaces to capture the induced micro- as well as the macro-textural features due to tire polishing. Similar method can be easily extended to analyze the induced the topological features on the on the pavement surfaces. Pavement surface texture can be thought of as a combination of microtexture and macrotexture. Friction between tire and road surface is strongly dependent on surface texture. Microtexture, in particular, plays a significant role in this interaction. In the previous sections, experimental texture measurements and DDS modeling methodology were introduced to analyze the polished and unpolished aggregate surfaces on AWI wear track. The elevation profiles collected from AWI wear track surface by a laser sensor were modeled and analyzed by use DDS methodology. Comparison of the modeling results leads to the following conclusions which are applicable to road pavement surface analyses.

1. Microtexture with a wavelength in the range of 0.1~0.5mm (which corresponds to the grain size of Port Inland aggregate) has a significant effect on the roughness of the aggregate surfaces. All the DDS modeling results for 1micron, 30micron and 45micron step size scans present the difference of microtexture between polished and unpolished aggregate surfaces.
2. For different step size scans, in order to obtain a consistent modeling results, different criteria have been adopted. For short scans, the dominant wavelength should be considered (when there is no overall slope in the elevation profile), but for longer scans the damping ratio criterion should be used.
3. Compared with other step size scans, 45 micron step size scan can capture both the macrotexture and the microtexture characteristics and can provide more texture information than other two scan sizes.
4. Since the unpolished surface is much more complex than the polished one, the modeling of the former surface requires a higher order of ARMA model than the latter.
5. The damping ratio criterion used in this paper is useful in microtexture analysis, especially for larger scan lengths. It will provide with the microtexture information, such as wavelengths and roughness resulting from DDS analysis.
6. Based on DDS analysis, the polishing effect due to traffic is to reduce the microtexture roughness of aggregate surfaces as well as the range of microtexture.

5. Investigation of road surface texture wavelengths

Pavement surface characteristics and traffic conditions are generally recognized as the major contributors to pavement friction. Statistic on pavement accidents indicates that each year approximately 15% of accidents that result in injury or fatality occurred during wet weather conditions. Some of these accidents resulted from loss of friction at the tire-pavement interface. The tire-pavement interaction has two contributions arising from adhesion and hysteric components. The adhesion term is interpreted as a thermally-activated molecular stick-slip action, which is described by a stationary stochastic process. The stationary stochastic process consists in the formation and breakage of adhesive linking chains that bind the rubber body to the textured surface (Schallamach, 1963; Chernyak and Leonow, 1986). The hysteric component results from the internal friction and subsequent dissipation of energy during cyclic deformation of sliding rubber arising from the asperities of rough substrate which exerting oscillating forces on the rubber surface. Kummer (1966) proposed a model for rubber friction that considered the above two components of the friction: the adhesion component based on microtexture and the hysteresis component based on the macrotexture. Persson (1998) qualitatively presented that the hysteric contribution was associated with the long wavelength roughness of substrate. The interaction between tire and substrate deformed the rubber so that it could 'follow' the short wavelength roughness of the substrate when the rubber slid at a low velocity. This deformation would provide an additional adhesion contribution to the friction. However, recent investigations indicated that for different type of tires, for example smooth and ribbed tires which are widely adopted for friction measurements on road surface, the friction measured on the same road surface will be significantly different. Generally the ribbed tire will present a higher friction and the smooth tire will result in a lower friction. Yandell and Sawyer (1994) pointed out that there was seldom agreement between any two different devices that measured friction on the same surfaces. For example, a runway friction tester and a pavement friction tester yielded an R-squared value of 0.02 for readings on about 25 wet open-graded textured roads using ribbed tires and an R-squared value of 0.75 on a large variety of wet asphalt surfaces using a smooth tire. Whitehurst (1978) also showed a 30 percent variation among seven different ASTM skid trailers reading identical surfaces. There are many reasons for this poor agreement, among which are the vagaries of tread rubber behavior. Due to the complexity of analysis in the tire characteristics of every vehicle to determine the friction between tire and road surface, it is imperative that pavement surfaces should be designed and constructed to provide adequate friction to minimize the accident rate as a result of frictional deficiencies.

Pavement texture is a feature of the road surface that ultimately determines most tire/road interactions, including wet friction, noise, splash and spray, rolling resistance and tire wear. The characteristics of pavement texture that affect tire and pavement interactions are arbitrarily categorized as microtexture, consisting of wavelengths (characteristic dimensions) of 1 μm to 0.5 mm, and macrotexture, consisting of wavelengths of 0.5 mm to 50 mm. It has been demonstrated that at low slip speeds the effect of microtexture dominates the friction measurement, whereas at high slip speeds the effect of macrotexture becomes important. Therefore, if both microtexture and macrotexture are maintained at high levels, they can provide sufficient resistance to skidding. A recent European study reports that increased macrotexture reduces total accidents, under both wet and dry conditions. Kokkalis (1998) also presented a relationship between wet pavement accident

rate and pavement macrotexture. As expected, when macrotexture increases, the accident rate is reduced. Fülöp et al. (2000) investigated the relationship between International Friction Index (IFI) and skid resistance and the relationship between IFI and surface macrotexture. They developed a relation that the IFI threshold value of friction is a function of the macrotexture parameter. The theoretical estimations corresponded well to their experimental results.

On the other hand, more and more researchers believe that microtexture has a substantial effect on skid resistance and various methods are proposed to evaluate microtexture. Forster (1994) conducted a study to investigate the quantitative role played by small-scale surface texture (microtexture) in determining the skid resistance of a pavement. A non contact image analysis system was used to measure the microtexture profiles on a series of pavement cores. The measurements of microtexture were correlated to the British Portable Tester numbers (BPNs) obtained on the same cores. A linear regression fit of these data based on 87 cores yielded a correlation coefficient (R-squared value) of 0.68. Do et. al. (2000) adopted the ideas from Fahl (1982) who emphasized that large profile peaks and valleys play an important role in functional applications and developed a 'theta angle' to measure the microtexture of road surface. The 'theta angle' was derived from the two consecutive peaks and the horizontal between every segment on road surface profile. The theta angle distribution was used to characterize the microtexture roughness. Correlation between theta values and friction gave a correlation coefficient R-squared value of 0.8 for 24 data points. Rohde (1976) demonstrated the importance of microtexture pattern as well as its amplitude on the load-carrying capability and the descent time of the tread element. Persson and Tosatti (2000) presented a comprehensive treatment of the hysteric contribution to the friction for viscoelastic solids sliding on hard substrates with different types of (idealized) surface roughness. They found that, when rubber is slowly sliding on the surface, at velocity less than 1cm/s (as in the case to ABS-braking of automotive tires on dry and wet road surface), the rubber will deform and fill out the nanoscale cavities associated with the short-ranged surface roughness and this gives an additional contribution to the sliding friction. Huang (2010) utilized Data Dependent Systems (DDS) approach to model and analyze the elevation profiles collected from polished and unpolished aggregate surfaces of Aggregate Wear Index (AWI) wear track. It was revealed that the microtexture roughness of aggregate surfaces was influenced significantly by tire polishing effect and the DDS approach was able to capture both the characteristics of microtexture and macrotexture.

Due to the vital role of pavement texture in both pavement friction and tire wear, Michigan Department of Transportation (MDOT) initiated a research program of pavement texture analysis in the Center of Transportation Materials Research at Michigan Technological University. As the second part of this research program, the current work presents a texture analysis from several bituminous pavement surfaces obtained from Michigan. A total 212 road surface cores from 29 sites on suburban and rural lanes were obtained. From each site, samples of 6 inch diameter were cored from shoulder, both wheel paths and between wheel paths. A laser profilometer was used to collect elevation profiles on each core. The Data Dependent Systems (DDS) methodology (Pandit, 1991) was introduced to model and analyze the elevation profiles. Similar to the previous investigations on the aggregate surfaces of AWI wear track, 1 micron and 45 micron step sizes were chosen to measure the texture. A total of 1,024 readings were taken per individual line scan along the traffic direction. For bituminous pavement, skid resistance gradually decreases by the polishing action of traffic. A generally accepted explanation concerning the reduction process is that

traffic abrades the pavement surface, exposing the aggregate and makes aggregate worn and polished which, in turn, reduces skid resistance. Therefore, polishing properties of coarse aggregates play a significant role in determining skid resistance. On the other hand, the 4th section in this article utilized the DDS methodology analyzing the tire polishing characteristics of aggregate surface on AWI wear track and found that the tire polishing process will mainly affect the microtexture of aggregate surfaces. Based on the above analyses, 1 micron step size scan was used to collect the elevation profile from exposed aggregate on each core surface. To collect the data randomly on any given core, a five by five grid of points was applied to an area of 25 cm^2 on each core surface. This eliminates any bias in the location of region from where the data was collected. The 1 mm long scan was collected closest to each grid point and a total 25 scans were obtained on each core. For the 45 micron step size, since DDS modeling can capture both the characteristics of macro- and micro-texture, the texture data collection included a series of twelve – 46 millimeter long linear traverses collected from an area of 100 cm^2 on each core surface for a total traverse length of approximately 552 mm. The characteristics of both microtexture and macrotexture reflected surface feature of pavement core were correlated to the British Pendulum Tester numbers (BPNs) and the Laboratory Friction Tester values (LBF) obtained on the same core.

6. Data analysis and correlation of DDS analysis with BPN value

Based on the DDS theory, the collected data from core surfaces were analyzed using DDS program. Since it was difficult to find an apparently physical parameter as an additional criterion to determine an adequate model from most of core surfaces, only the independence of the residuals (the a_t 's) and the F-test criterion were applied to find an adequate model for each scan.

6.1 Modeling analyses of 1 micron step size scans

Microtexture is a measure of the degree of polishing of a pavement surface or of the aggregate at the surface. It has been realized that microtexture is dependent primarily upon the aggregate petrographic characteristics and the traffic intensity (expressed in terms of commercial-vehicle flows). It is clear that at different stages of a pavement's service life the aggregate surface presents different texture profiles. For example, in the early stage of a pavement service, the influence of an aggregate's polishing characteristics on skid resistance is thought to be minimal because the bituminous matrix has not been worn sufficiently to expose the aggregate. But in the later stage of the pavement service, aggregate surface texture is essential to sustain the skid resistance of the pavement. Therefore, the elevation profiles of aggregate surface may, to some extent, represent the variation of road surface friction and the 1 micron step size scan is adopted to correlate the aggregate surface texture with pavement surface friction. In the this paper, the DDS analysis of 1 micron step size scan is correlated with the British Pendulum Tester numbers (BPN) and Laboratory Friction Tester values (LBF) obtained from the same pavement core, respectively.

The BPN has been wildly used in laboratory and field testing of frictional properties of surfaces. The BPN value measured by the tester represents the amount of kinetic energy lost when a rubber slider attached to the end of a pendulum arm is propelled over a test surface. Many researchers have proved that BPN value has a good correlation with the microtexture measurements. The laboratory friction tester (LBF) was built in a laboratory of Michigan Department of Transportation (MDOT). It is a companion friction tester for the circular

Aggregate Wear Index (AWI) wear track. It can measure an initial peak drag force as a test tire comes into contact with specimen at a special velocity. More details about LBF tests can be found in the paper of Dewey, et al. (2002). The BPN and LBF data were obtained in house by MDOT from all the 212 road surface cores. Figure 6 presents a correlation between BPN and LBF. A very good correlation can be found between BPN and LBF test values (The coefficient of correlation (R^2) is 0.9081).

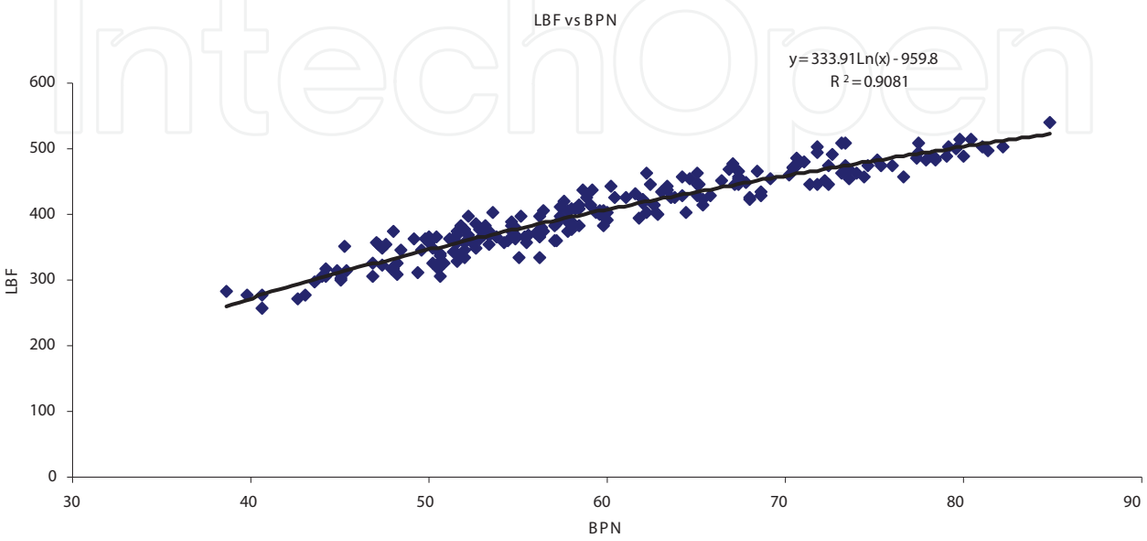

Fig. 6. Correlation between BPN and LBF for all cores

After an adequate model is obtained, the DDS model provides frequency (refers to number of cycles per millimeter), wavelength (is simply the inverse of this spatial frequency), damping ratio (indicates how well a given wavelength component of the profile repeats at that frequency) and contribution (is the averaged squared deviation from a mean height). Generally in an elevation profile, there always exists a dominant peak that represents the largest contribution and the largest wavelength compared to other wave crests or wave troughs and is called dominant contribution. The dominant peak may not repeat in the same elevation profile and will show up as a real root with large wavelength in DDS analysis. In the previous section of this paper, the DDS approach has been utilized to investigate the characteristics of polished and unpolished aggregate surfaces. It was found that for both polished and unpolished aggregate surfaces, the dominant contributions almost all came from real roots and the corresponding wavelengths are attributed to the microtexture. Since the dominant contribution is much larger than other contributions in each scan, it dominates the value of variance and this leads the variances to have the same trend as the dominant contributions. Therefore, the correlation of variances with BPN or LBF is explored for 1 micron step size scan.

Figure 7 and 8 present a correlation between the calculated variances versus BPN values and LBF values for all the 212 pavement surface cores, respectively. The variance data in these figures is obtained by summing the variances from all scans on a given core, and then averaging it. A nearly linear trend can be found from the two figures and LBF values have a slight better correlation with the surface roughness variances than BPN values have. In Figures 7 and 8, since the values of variances are very small (those values are scattered over

the range of around 10^{-1} to 10^{-4}) and the variance has units of squared length we have used the square root of variance to further improve the correlations. Moreover the square root of variance has a physical meaning that indicates the averaged roughness of pavement surface with a length unit. Figures 9 and 10 present the correlations with BPN and LBF. The square root of variance is calculated by obtaining the square root of variance from every scan, adding them up for a given core and then averaged for all the scans. Comparing to the Figures 7 and 8, Figures 9 and 10 do show a better correlation. The correlation coefficients (R^2) increase from 0.091 to 0.1962 for BPN and from 0.1227 to 0.2471 for LBF. It can be found again that LBF has a higher R^2 than BPN.

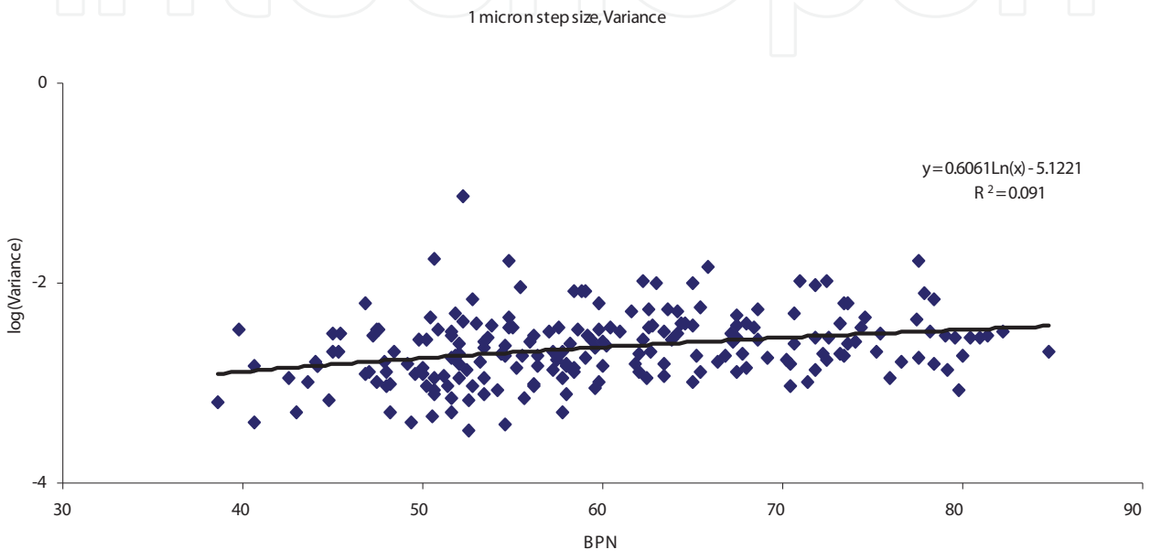

Fig. 7. Correlation between variance and BPN for all cores

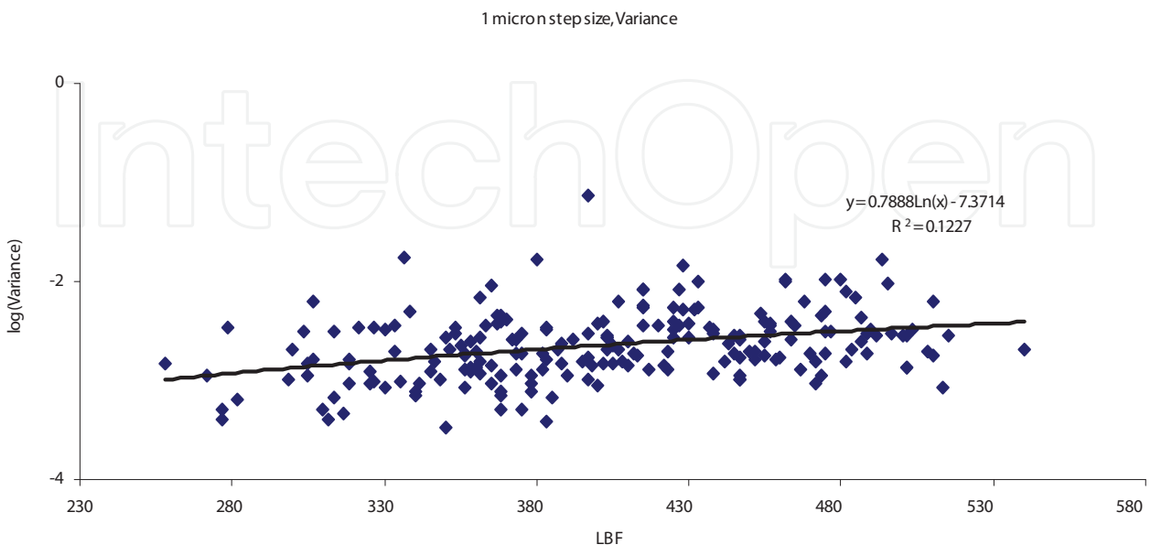

Fig. 8. Correlation between variance and LBF for all cores

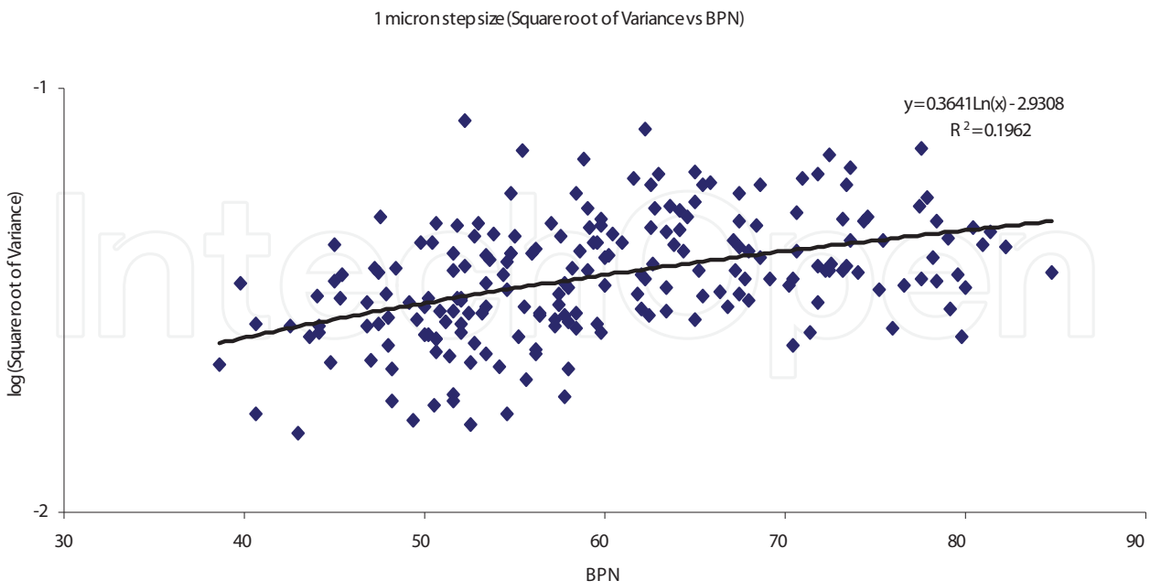

Fig. 9. Correlation of square root of variance with BPN for all cores

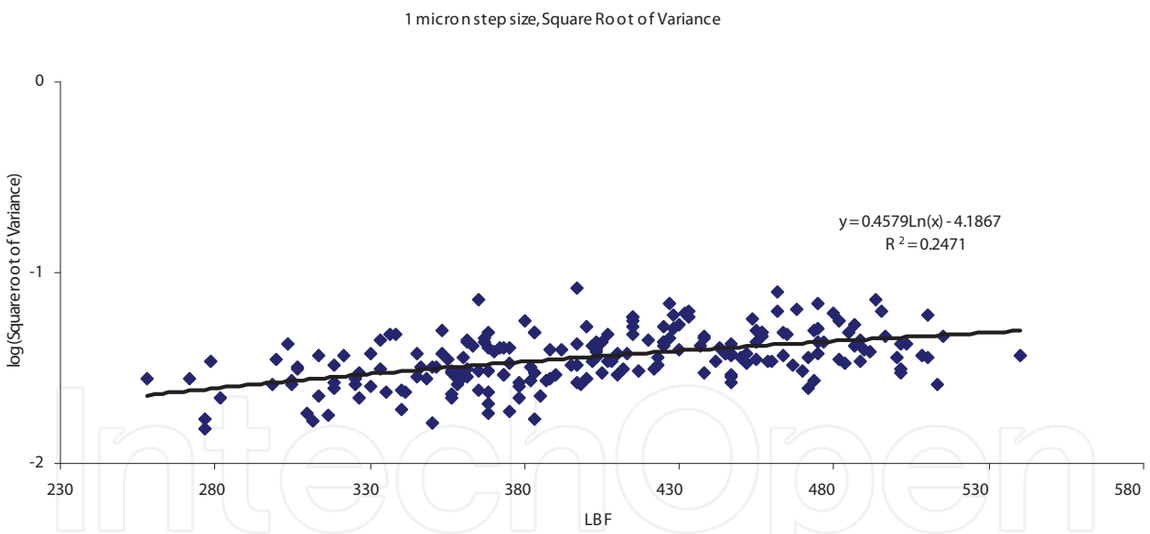

Fig. 10. Correlation of square root of variance with LBF for all cores

In the above plots all the pavement surface samples including those cored from shoulder, both wheel paths and between wheel paths were included. However, those cores from shoulder and between wheel paths are seldom polished by vehicle tire and hence may affect the correlation of the aggregate roughness with BPN and LBF values. In order to explore the effect of tire polishing on road surface friction, Figure 11 and Figure 12 present those variance data collected only from the samples that were cored from both wheel paths. This reduces the total number of cores to 116. Figures 11 and 12 exhibit the correlation of square root of variance from wheel path cores with BPN and LBF. Compared to the correlation with all the cores presented in Figures7 and 8, the correlation with wheel path cores has a better

coefficient of correlation, which indicates that the correlation of aggregate roughness with BPN and LBF is really affected by the vehicle tire polishing and, to some extent, the averaged aggregate roughness (square root of variance) does exhibit a relationship with the skid resistance of road surface. On the other hand, we explored some other contributions related to very short wavelengths by damping ratio criterion (see next section for detail of the criterion) and correlated them with BPN and LBF values based on total cores and wheel path cores, respectively. None of these measures gave good correlations.

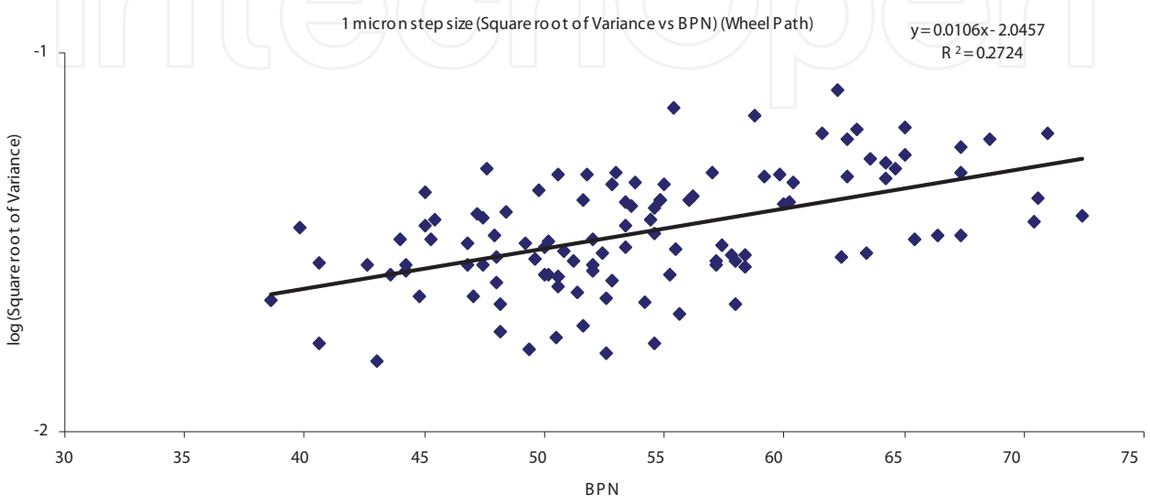

Fig. 11. Correlation of square root of variance with BPN for wheelpath

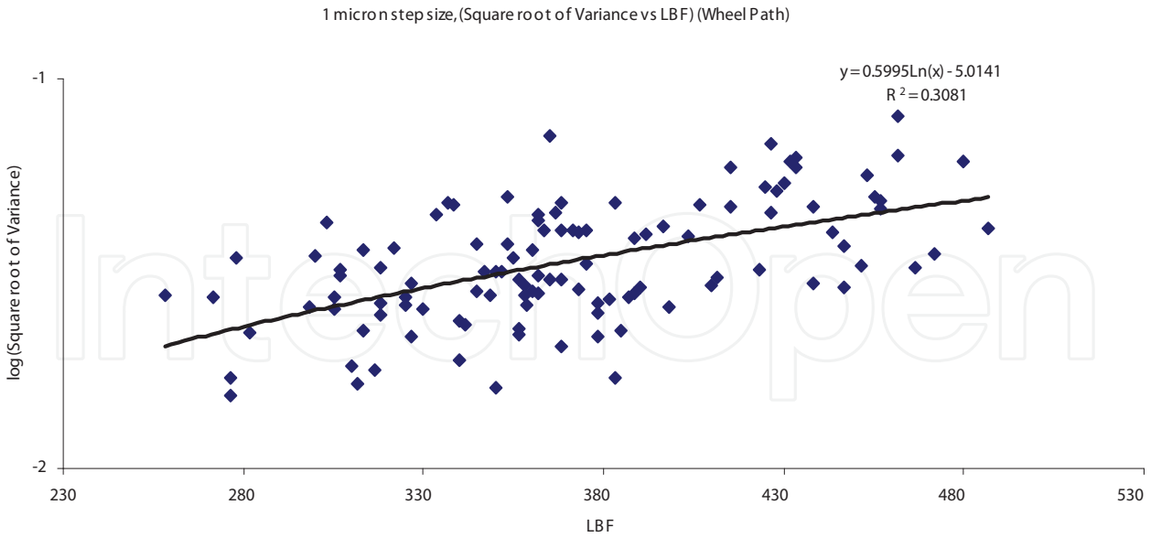

Fig. 12. 7 Correlation of square root of variance with LBF for wheelpath

6.2 Modeling analyses of 45 micron step size scans

Although the 1 micron step size scans collected from aggregate surfaces on road pavement cores present a correlation with pavement skid resistance, it is still necessary to explore a

correlation between the pavement surface texture and pavement skid resistance. Because the aggregate surfaces just can provide with microtextural information to correlate with skid resistance, more information about the macrotexture of pavement surface need to be explored.

In the previous section, the 45 micron step size scan, which spans over a length around 46mm, has been found to be a good measurement for the characterization of macro- as well as micro-texture. For most of 45 micron step size scans, the dominant real roots usually present the characteristics of macrotexture and the characteristics of microtexture can be captured by using damping ratio criterion. Similar to the situation in 1 micron step size scans, the dominant contribution is much larger than other contributions in most of scans, so variance should have the same trend as the dominant contribution and represents the characteristics of macrotexture. The damping ratio criterion used here is that when the damping ratio is less than 13%, the corresponding contribution will be selected and then summed over all the contributions that satisfy this damping ratio criterion to obtain a partial contribution in one scan. For any given pavement core, there are twelve elevation scans collected from its surface so a total 12 partial contributions are summed up and then averaged to gain a partial contribution value for the given core. Since most of the wavelengths satisfying the damping criterion are less than 0.5mm, the texture can be depicted as microtexture and the associated partial contributions physically describe the averaged square deviation of microtexture roughness.

Table 10 presents the correlation between DDS analysis and road surface friction BPN and LBF. In Table 10 the numbers represent the coefficients of correlation (R^2), The variance or square root of variance does not have a correlation with either LBF or BPN. It implies that it is almost impossible to correlate macrotexture with road surface friction in 45 micron step size scans. In other words we could not find the correlation between macrotexture measures and road surface friction by the simple variance analysis or the dominant contribution analysis of DDS approach. On the other hand, there dose exist a correlation between microtexture (which is expressed by partial contribution) and the two kinds of road surface friction. One interesting phenomenon is that the correlation with wheel path cores is less than the correlation with all the cores. This implies that the traffic polishing influence on microtexture of road surface matrix is not significant. Here, a question is raised, how can the polishing process of vehicle tire affect road surface matrix? Will it change the macrotexture or something else?

Table 11 presents the correlations of contributions that satisfy a new wavelength criterion with the two kinds of road surface friction. The wavelength criterion is that for every scan a special wavelength is prescribed, if a wavelength is equal to or less than the prescribed wavelength, the corresponding contribution will be picked and then summed up to gain a partial contribution based on the scan, which represents the averaged square roughness corresponding to the prescribed wavelength. For a given core, sum up all the partial contributions coming from all the scans on the given core and then average them based on the scan number. Four scale wavelengths are chosen, they are 0.5, 1.0, 1.5 and 2.0 mm. From the Table 11, when wavelength $\lambda \leq 1.0$ mm, it will have the highest coefficient of correlation with the two kinds of friction and those two values are close to the coefficients of correlation values we found in 1 micron step size scans. Therefore, the polishing process of vehicle tire will mainly affect the 1 mm wavelength texture on road surface matrix. It should be pointed out that bituminous pavement surfaces in our analysis all belong to mixed types of pavement, they are composed of different compositions, such as different kind of aggregates and different size of aggregates. The type of mixed bituminous pavement has exhibited a significant influence on

the correlation of pavement surface texture with road surface friction tests. Table 12 and 13 presented those coefficients of correlation between DDS analysis and friction tests for 1 micron and 45 micron step size based on different mixed type surface, respectively.

In Table 12, SQRT(variance) means square root of variance, the square root of variance was obtained from each scan and then was averaged based on each pavement core. mixtype 4 that it was mainly composed of sand and gravel (SG) and had the maximum aggregate size around 12.5mm, has the highest coefficient of correlation with BPN and LBF (the coefficients of correlation (R^2) are 0.5335 and 0.5167, respectively). Therefore, the aggregate profile on this type of pavement surface can be correlated well with friction tests. Mixtype SMA has the second place for the correlation with friction test. SMA was generally composed of SG (43%) and carbonate (57%) and the maximum aggregate size was around 19mm. The poorest coefficients of correlation with friction were mixtype Micro and Slag. It is realized that pavement constructed by slag aggregate usually has no correlation with friction test based on the characteristics of slag. So it is not surprising to obtain a poor correlation for slag pavement in terms of DDS analysis.

Table 13-1 and 13-2 present the correlation of pavement surface texture with friction for 45 micron step size scan analysis. SQRT(partial) indicates the square root of partial contribution and negative values represents an inverse trend. The partial contribution is obtained in terms of the above damping ratio criterion and is calculated based on each scan and is averaged for a given pavement core. In the tables, the column of SQRT(variance) has a weak correlation with both the friction tests for different types of mixtype pavement. It proves again that variance of elevation profile is not an appropriate description for surface texture to correlate with road surface friction. This conclusion is also consistent with the results we obtained in Chapter 2. When the surface texture wavelength is equal to or less than 1mm, mixtype SMA has the highest coefficient of correlation with friction BPN and LBF. For mixtype Micro, different from 1 micron analysis, it presents a good correlation with the frictions when wavelength varies from $\lambda \leq 2$mm, $\lambda \leq 1.5$mm, $\lambda \leq 1$mm, $\lambda \leq 0.5$mm and $\lambda < 0.5$mm (usually, the corresponding wavelengths satisfying the damping ratio criterion are always less than 0.5mm). Comparing Table 13-1 and 13-2, the wavelength $\lambda \leq 0.5$mm has the best correlation with the two friction tests (the R^2 values are 0.5498 with BPN and 0.4375 with LBF). For other mixtype road surfaces, mixtype 4 presents some trend with friction tests and mixtype Slag presents no trend with friction once again.

7. Conclusion

As a research subject, pavement texture has been widely studied for the past several decades. However, most of these research works were limited to characterizing the pavement surface texture qualitatively and are limited to either variance or RMS or MTD. Pavement surface texture has been generally accepted as a combination of microtexture and macrotexture. Friction between tire and road surface is considerably dependent on surface texture. In recent years, more and more researchers revealed that microtexture, in particular, plays a significant role in the road/tire contact friction. In this paper, experimental texture measurements and DDS modeling methodology were introduced to analyze the real road pavement surfaces obtained from Michigan. The elevation profiles collected from real road core surfaces were composed of 1 micron step size scan and 45 micron step size scan by an accurate laser sensor and were modeled by DDS program. Comparison of the modeling results, the following conclusions can be drawn.

1. Aggregate surface on real road pavement, to some extent, presents a correlation with road surface friction. For some mixtype (Such as Mixtype SMA, Mixtype 4 and Mixtype 13) pavements, the aggregate surface has a good correlation with friction tests, but for some mixtype does not.
2. The type of pavement has a significant effect on the correlation between surface texture and friction. Some types of pavement (such as Mixtype micro, Mixtype 4 and Mixtype SMA) present a strong correlation with friction, but some types do not exhibit the correlation with friction. And Mixtype 4 and Mixtype 13 have a consistent correlation from both aggregate surface and pavement surface matrix.
3. Variance of elevation profile is found to be an improper parameter to correlate with surface friction for large step size scan, such as 45 micro step size scan.
4. For some type of pavement, there exists a variation range of wavelengths where the corresponding roughness presents a good correlation with friction and these wavelengths are in the range of around 0.5mm to 2mm.
5. It is worth mentioning that there exist many factors that may affect the road surface roughness, such as the construction date, the amount of daily traffic, etc. After more factors that affect the surface roughness are considered, a better correlation of roughness with friction can be obtained.

Frequency Cycles/mm	Wavelength (mm)	Damping Ratio	Contribution (mm^2)	Variance (mm^2)
434	0.002306	3.09E-02	2.48E-08	2.25E-04
250	0.004006	3.19E-01	4.77E-07	
294	0.003403	4.49E-02	5.18E-08	
168	0.005956	2.40E-02	-1.04E-08	
9.94	0.100563	3.33E-01	2.37E-05	
500	0.002		9.90E-08	
2.31	**0.433839**		**2.01E-04**	

Table 1. DDS model results from a 1mm scan (01a) of a polished aggregate on AWI track

Frequency Cycles/mm	Wavelength (mm)	Damping Ratio	Contribution (mm^2)	Variance (mm^2)
466	0.002146	3.44E-03	1.51E-08	1.04E-03
217	0.004615	5.49E-02	-2.73E-08	
270	0.003711	4.75E-02	3.52E-09	
322	0.003102	5.09E-03	2.49E-10	
415	0.002410	2.37E-02	3.83E-08	
367	0.002727	1.18E-02	1.69E-08	
97.2	0.010288	6.77E-02	9.44E-08	
112	0.008947	2.77E-01	-3.30E-07	
7.02	0.14245	7.22E-01	-3.80E-04	
93.2	0.010725	1.16E-06		
193	0.005195	5.63E-02	-2.63E-08	
2.69	**0.372024**	**1.42E-03**		

Table 2. DDS model results from a 1mm scan (011) of an unpolished aggregate on AWI track

Scan ID		Variance (mm^2)		Dominant Wavelength (mm)		Dominant Contribution (mm^2)	
Polished	Unpolished	Polished	Unpolished	Polished	Unpolished	Polished	Unpolished
01a	011	2.25E-4	1.04E-3	0.4338395	0.3720238	2.01E-4	1.42E-3
01b	012	7.24E-5	2.75E-3	0.1930502	0.1228199	6.40E-5	2.73E-3
01c	013	1.14E-4	7.86E-4	0.2016536	0.2457606	1.13E-4	7.83E-4
01d	014	2.66E-4	5.42E-4	0.2810568	0.307031	2.65E-4	8.67E-4
01e	015	4.65E-5	1.41E-3	0.2644803	0.4299226	4.47E-5	2.72E-3

Table 3. Comparison of polished and unpolished Surfaces Modeling (1micron)

Frequency Cycles/mm	Wavelength (mm)	Damping Ratio	Contribution (mm^2)	Critetion (mm^2)	Partial (mm^2)	Variance (mm^2)
2.10	0.477	2.84E-01	2.60E-04		1.013E-5	8.48E-4
8.70	0.115	3.49E-02	-1.17E-06	-1.17E-06		
12.0	0.084	1.84E-02	3.30E-03	3.30E-07		
16.7	0.060		3.60E-05			
5.54	0.181	6.92E-03	1.10E-05	1.10E-05		
0.597	**1.674**		**5.28E-04**			
10.8	0.093	3.64E-01	1.44E-05			

Table 4. 30a Polished Scan

Frequency Cycles/mm	Wavelength (mm)	Damping Ratio	Contribution (mm^2)	Critetion (mm^2)	Partial (mm^2)	Variance (mm^2)
5.09	0.196	6.11E-02	2.89E-05	2.89E-05	1.80E-4	6.85E-2
15.0	0.067	3.81E-03	5.70E-07	5.70E-07		
11.4	0.087	8.60E-02	-4.38E-06	-4.38E-06		
9.44	0.105	9.36E-03	-1.84E-08	-1.84E-08		
1.96	0.510	2.39E-01	3.15E-05			
0.773	1.293		6.56E-05			
7.04	0.142	6.54E-02	3.09E-05	3.09E-05		
4.10	0.244	8.29E-03	1.24E-04	1.24E-04		
12.7	0.079	7.98E-03	-3.47E-07	-3.47E-07		
0.012	**82.44**		**6.83E-02**			
14.1	0.071	2.36E-01	-1.26E-05			

Table 5. 301 Unpolished Scan

Scan ID		Variance (mm²)		Microtexture Wavelength Range (mm)		Partial Contribution (mm²)	
Polished	Unpolished	Polished	Unpolished	Polished	Unpolished	Polished	Unpolished
30a	301	8.48E-04	6.85E-02	0.08~0.18	0.07~0.24	1.01E-05	1.80E-04
30b	302	2.66E-03	9.82E-03	0.07~0.16	0.07~0.76	1.70E-05	1.05E-04
30c	303	1.21E-03	2.24E-03	0.09	0.07~0.66	-3.62E-07	1.60E-04
30d	304	2.17E-03	1.84E-02	0.08	0.07~0.23	-2.80E-06	1.54E-04
30e	305	4.58E-04	1.77E-02	0.15	0.07~0.4	1.21E-05	1.34E-04

Table 6. Comparison of Polished and Unpolished Surfaces Modeling (30micron)

Frequency Cycles/mm	Wavelength (mm)	Damping Ratio	Contribution (mm²)	Critetion (mm²)	Partial (mm²)	Variance (mm²)
0.0961	**10.4**	**4.40E-01**	**1.46**		-5.35E-07	1.46
6.56	0.153	3.25E-02	-5.35E-07	-5.35E-07		
5.31	0.188		-4.96E-03			
11.1	0.09		-1.67E-05			

Table 7. c45 Polished Scan

Frequency Cycles/mm	Wavelength (mm)	Damping Ratio	Contribution (mm²)	Critetion (mm²)	Partial (mm²)	Variance (mm²)
11.1	0.09		-7.55E-04		8.143E-04	0.636
2.12	0.47	2.76E-02	2.05E-04	2.05E-04		
5.89	0.17	1.88E-03	9.08E-06	9.08E-06		
7.57	0.13	2.34E-02	-9.83E-06	-9.83E-06		
9.86	0.10	3.61E-03	2.04E-06	2.04E-06		
3.81	0.26	3.84E-02	1.86E-04	1.86E-04		
11.1	0.09		2.34E-06			
2.98	0.34	4.78E-02	4.21E-04	4.21E-04		
0.15	**6.64**	**4.74E-01**	**6.36E-01**			

Table 8. w45 Unpolished Scan

Scan ID		Variance (mm²)		Dominant Wavelength (mm)		Partial Contribution (mm²)		Microtexture Wave-length Range (mm)	
Polished	Unpolished	Polished	Unpolished	Polished	Unpolished	Polished	Unpolished	Polished	Unpolished
A45	V45	0.336	0.463	4.7	6.14	-9.23E-6	5.44E-4	0.153	0.1~0.37
B45	W45	2.03	0.723	5.26	7.53	1.3E-4	5.37E-4	0.1~0.22	0.1~0.47
C45	X45	1.46	0.636	10.4	6.64	-5.35E-7	8.14E-4	0.1~0.14	0.1~0.47
D45	Y45	0.247	1.55	15.74	5.68	1.26E-5	1.19E-3	0.1~0.23	0.1~0.37
E45	Z45	0.697	0.999	3.9	9.41	-4.65E-5	7.02E-4	0.1~0.13	0.1~0.32

Table 9. Comparison of Polished and Unpolished Surfaces Modeling (45micron)

	BPN		LBF	
	All cores	Wheel Path cores	All cores	Wheel Path cores
Variance (mm^2)	0.0044	No trend	0.0015	No trend
Square root of variance (mm)	0.0104	No trend	0.0059	No trend
Partial contribution (mm^2)	0.1395	0.1156	0.1333	0.101

Table 10. Correlation between DDS analysis and road surface friction

	Contributions satisfy wavelength λ (mm) criterion			
	$\lambda \leq 0.5$	$\lambda \leq 1.0$	$\lambda \leq 1.5$	$\lambda \leq 2.0$
BPN	0.1769	0.2455	0.1187	0.1408
LBF	0.0766	0.2837	0.0362	0.1564

Table 11. Polishing influence on wavelengths of road surface texture

Core Types	Coefficient of correlation (R^2)			
	BPN		LBF	
	variance	SQRT (variance)	variance	SQRT (variance)
All cores	0.0842	0.1835	0.1187	0.2383
Wheel path cores	0.1542	0.2742	0.1763	0.3142
Mixtype Micro	0.0086	0.0377	0.0015	0.0027
Mixtype SMA	0.2589	0.3484	0.1858	0.2263
Mixtype 13	0.1325	0.1695	0.1964	0.221
Mixtype 4	0.3434	0.5335	0.3281	0.5167
Mixtyp SLAG	0.0122	0.0298	0.0355	0.0959

Table 12. Correlations between core types and surface measures for 1 micron step size

Core Types	Coefficient of correlation (R^2)					
	SQRT (variance)	SQRT(Partial)	$\lambda \leq 0.5$	$\lambda \leq 1.0$	$\lambda \leq 1.5$	$\lambda \leq 2.0$
Wheel path cores	0.0613	0.1461	0.1769	0.2455	0.1187	0.1408
Mixtype Micro	0.1264	0.4198	0.5498	0.4672	0.6319	0.5209
Mixtype SMA	0.2198	0.4553	0.5027	0.7122	0.6569	0.585
Mixtype 13	0.0929	0.0291	0.0001	0.0068	0.0016	0.0038
Mixtype 4	0.0015	0.2879	0.1575	0.1057	0.0575	0.048
Mixtyp SLAG	0.1212	0.0021	0.0575	0.0715	0.0905	0.0777

Table 13-1. Correlations between BPN and surface measures for 45 micron step size

Core Types	Coefficient of correlation (R^2)					
	SQRT (variance)	SQRT (Partial)	$\lambda \leq 0.5$	$\lambda \leq 1.0$	$\lambda \leq 1.5$	$\lambda \leq 2.0$
Wheel path cores	0.0603	-0.002	0.0766			
Mixtype Micro	0.2969	0.3399	0.4375	0.2837	0.0362	0.1564
Mixtype SMA	0.0391	0.1205	-	0.2544	0.2032	0.2023
Mixtype 13	0.0792	0.0595	0.00000	0.4417	0.008	0.2179
Mixtype 4	0.0136	0.345	1	0.0272	-0.2499	-
Mixtyp SLAG	0.0299	0.0526	-0.1503	0.2407	0.0752	0.00009
			0.0073	0.2246	0.2114	0.1588
			0.2446			0.2072

Table 13-2. Correlations between LBF and surface measures for 45 micron step size

8. Reference

Chernyak, Yu. B. and A. I. Leonov (1986), On the theory of the adhesive friction of elastomers, Wear 108,105-138

Dewey, G. R., A. C. Robords, B. T. Armour and R. Muethel (2001), Aggregate Wear and Pavement Friction, *Transportation Research Record*, Paper No. 01-3443.

Do, M. T., H. Zahouani and R. Vargiolu (2000), Angular parameter for characterizing road surface microtexture. In Transportation Research Record 1723, TRB, National Research Council, Washington, D. C., 66.

Fülöp, I. A., I. Bogárdi, A. Gulyás and M. Csicsely-Tarpay (2000), Use of friction and texture in pavement performance modeling, *J. of Transportation Engineering*, 126(3), 243-248.

Gunaratne, M., M. Chawla, P. Ulrich and N. Bandara (1996), Experimental investigation of pavement texture characteristics, *SAE 1996 Transactions Journal of Aerospace*, 105(1), 141-146.

Kokkalis, G. (1998), Prediction of skid resistance from texture measurements, Proc. Instn Civ. Engrs Transp., 129, 85-.

Kummer, H. W., Unified theory of rubber friction, Engrg. Res. Bull. B-94, Penn State University, State College, University Park, Pa., (1966)

Pandit, S. M. and S. M. Wu (1983), *Time series and system analysis with applications*, John Wiley.

Pandit, S. M. (1991), *Modal and Spectrum Analysis: Data Dependent Systems in State Space*, Wiley Interscience.

Perera, R. W., S. D. Kohn and S. Bemanian (1999), Comparison of road profilers, *Transportation Research Record*, 1536, 117-124.

Persson, B. N. J. and E. Tosatti (2000), Qualitative theory of rubber friction and wear, *Journal of Chemical Physics*, 112(4), 2021-2029.

Rohde, S. M. (1976), On the effect of pavement microtexture and thin film traction. *Int. J. Mech. Sci*., 18(1), 95-101.

Taneerananon, P. and W. O. Yandell (1981), Microtexture roughness effect on predicted road-tire friction in wet conditions, *Wear*, 69, 321-337.

Schallamach, A. (1963), Wear 6, 375

Yandell, W. O. and S. Sawyer (1994), Prediction of tire-road friction from texture measurements, Transportation Research Record 1435, Transportation research Board, National Research Council, washinton D. C..

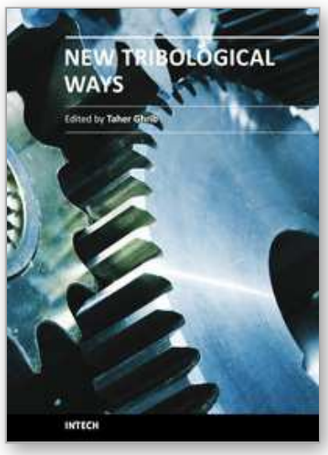

New Tribological Ways

Edited by Dr. Taher Ghrib

ISBN 978-953-307-206-7
Hard cover, 498 pages
Publisher InTech
Published online 26, April, 2011
Published in print edition April, 2011

This book aims to recapitulate old information's available and brings new information's that are with the fashion research on an atomic and nanometric scale in various fields by introducing several mathematical models to measure some parameters characterizing metals like the hydrodynamic elasticity coefficient, hardness, lubricant viscosity, viscosity coefficient, tensile strength .... It uses new measurement techniques very developed and nondestructive. Its principal distinctions of the other books, that it brings practical manners to model and to optimize the cutting process using various parameters and different techniques, namely, using water of high-velocity stream, tool with different form and radius, the cutting temperature effect, that can be measured with sufficient accuracy not only at a research lab and also with a theoretical forecast. This book aspire to minimize and eliminate the losses resulting from surfaces friction and wear which leads to a greater machining efficiency and to a better execution, fewer breakdowns and a significant saving. A great part is devoted to lubrication, of which the goal is to find the famous techniques using solid and liquid lubricant films applied for giving super low friction coefficients and improving the lubricant properties on surfaces.

InTech Europe
University Campus STeP Ri
Slavka Krautzeka 83/A
51000 Rijeka, Croatia
Phone: +385 (51) 770 447
Fax: +385 (51) 686 166
www.intechopen.com

InTech China
Unit 405, Office Block, Hotel Equatorial Shanghai
No.65, Yan An Road (West), Shanghai, 200040, China
中国上海市延安西路65号上海国际贵都大饭店办公楼405单元
Phone: +86-21-62489820
Fax: +86-21-62489821

IntechOpen